ORIGINAL PAPER

Xiaohua Zou · Song Zhang · Mianhong Shi · Jilie Kong

Remarkably enhanced capacitance of ordered polyaniline nanowires tailored by stepwise electrochemical deposition

Abstract A stepwise deposition method was employed to create ordered polyaniline (PANI) nanowires with remarkably enhanced capacitance. Cyclic voltammetry, AC impedance, and galvanostatic charge/discharge cycling were employed to investigate the electrochemical performance of the PANI electrodes. The PANI-deposited electrode exhibits much higher capacitance than those prepared by one-step deposition method, which were mainly contributed from the unique nano structure of PANI and the increased biological, economical, and technical surface areas. The superior capacitive behaviors of the nano PANI electrodes show great potential in preparation of high efficient electrochemical capacitors or rechargeable batteries.

Keywords Capacitance · Polyaniline · Nanowires

Introduction

In the past two decades, the electrochemical capacitor has drawn much attention for its higher power rechargeable batteries and its higher energy storage than conventional capacitors. Many materials, such as carbon fiber or nanotubes [1–4], ruthenium oxide [5–8], and conducting polymers [9–15], were extensively studied for the goal of enhancing the capacity and the stability of the capacitors. Among them, polyaniline (PANI) [16, 17] attracted particular attention due to its potential applications in high efficient energy storage systems with low cost and easy preparation, which would overcome the disadvantages of low capacity of carbon and high cost of noble metal oxide. Normally, PANI electrodes were prepared by galvanostatic, potentiostatic, and potentiodynamic methods. The deficiency of these routine methods was regarded that the structure of the formed polymer could not be controlled to create a desired ordered pattern, which would strongly limit

the final capacitance yield. This may be the reason why most of the reported PANI-based materials possess capacitances less than 200 F/g [10–13].

Considering that the material with oriented microstructure and high porosity would provide a higher surface area and thus may favor ions accessing from the electrolyte into the electrode surface [3], which would then consequently enhance the capacitance to some extent, we decided to pursue an innovative way to optimize the performance of PANI-based electrochemical capacitors. Recently, Liu et al. [18] reported a novel stepwise electrochemical deposition strategy by which large arrayed uniform and oriented nanowires of conducting PANI was formed without using any supporting porous templates to confine the polymers and in turn applied in the preparation of biosensors. Motivated by this pioneer work, here we employed similar three-step approach to create ordered PANI nanowires on platinum, gold, and carbon substrates with unique ordered 3-D structures as novel electrode materials. The electrochemical properties of these PANI supercapacitors were investigated by cyclic voltammetry (CV), AC electrochemical impedance spectroscopy, and galvanostatic charge/discharge cycling techniques.

Experimental

Materials

Reagent grade aniline (HUSHI Chemical, Shanghai, China) employed in the present work was distilled twice and the resulting colorless liquid was kept under nitrogen in darkness at 3°C. All the other reagents used in this work were also reagent grade and supplied by HUSHI and were used without pretreatment.

Preparation of PANI films

A standard three-electrode cell was used for the preparation of films and the subsequent electrochemical measurements. A saturated calomel reference electrode (SCE) and a glass-

X. Zou · S. Zhang · M. Shi · J. Kong (✉)
Department of Chemistry, Fudan University,
Shanghai 200433, People's Republic of China
e-mail: jlkong@fudan.edu.cn

carbon electrode were used as the reference and the counter electrode. Platinum (Pt) membrane, gold (Au) membrane, and carbon (C) electrodes were used as working electrodes.

The polymerization of PANI was performed by two experimental protocols as in Scheme 1, i.e., via three-step and one-step methods under nitrogen atmosphere. An electrolyte solution with 0.5 M H_2SO_4 and 0.5 M aniline was used for polymerization. In the three-step method, polyaniline was grown on the surface of Pt, Au, and C by redox polymerization of aniline using a programmed constant-current method designed to control the nucleation and growth rate. The optimized procedure was set at 0.02 mA cm^{-2} for 0.5 h followed by 0.01 mA cm^{-2} for 3 h, and another 8 h at 0.005 mA cm^{-2}. As a control experiment, the conventional one-step method (constant-current method) was performed by applying 0.02 mA cm^{-2} for 4 h when the total mass of the formed PANI is almost equal to that by three-step method, 0.28 mg/cm^2, calculated from the deposition charge Q via $m = Q \times MW/F$.

Surface configuration characterization

Surface morphologies of these polymer films were examined by Scan Electron Microscope (Philip XL 30). PANI used for the measurement was synthesized on Pt membrane, Au membrane, and C electrodes by the three-step and one-step methods.

Electrochemical measurement

Electrochemical measurements (CV, AC impedance, and galvanostatic charge/discharge cycling) were carried out at ambient temperature using 0.5 M H_2SO_4 aqueous solution as electrolyte to examine the electrochemical performance of PANI electrodes. All electrochemical measurements were carried out in a three-compartment cell. PANI electrode of different substrates was used as the working electrode. A glass-carbon electrode was used as the counter electrode. SCE was used as the reference electrode.
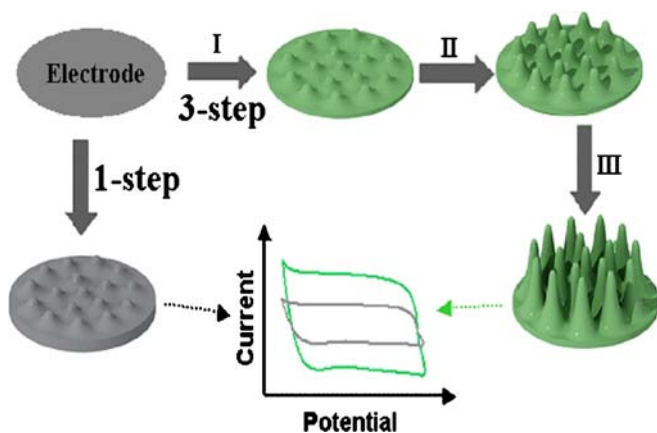
Scheme 1 The idealized cartoon for the preparation of PANI films via three-step and one-step methods. The inserted CV illustrated the corresponding capacitive behaviors for these two cases

CHI 660 (CH Instrument, USA) was used for CV and galvanostatic charge/discharge cycling of these polymer films. For the cyclic voltammetric measurements, the potential scan rate was 5 mV/s within the potential range of 0.1 to 0.7 V. Constant current charge/discharge cycling was performed with constant charge/discharge current density of 1 mA cm^{-2} between 0 and 0.7 V for 1,000 cycles. Potentiostatic/ galvanostatic model M-273 (Princeton) was employed to measure the AC-impedance spectra. The potential perturbation amplitude was fixed at 5 mV in the open-circuit potential and frequencies varied from 100 kHz to 10 mHz.

BET analysis

Biological, economical, and technical (BET) surface area was measured by Micromeritics Tristar ASAP 3000 v3.00. PANI used for the measurement was synthesized by the three-step and one-step methods as follows: a Pt electrode of 38 cm^2 was used as working electrode. A Pt screen electrode (48 cm^2) and an SCE were used as the counter and reference electrode. An electrolyte solution with 0.5 M H_2SO_4 and 0.5 M aniline was used for polymerization.

Results and discussion

SEM micrographs of PANI via three-step and one-step methods

The morphology of the prepared PANI films formed on the Pt, Au, and carbon substrates either by three-step or one-step growth was examined under SEM as shown in Fig. 1. As displayed in Fig. 1, unique and oriented PANI films consisting of ordered nanowires were obviously formed via
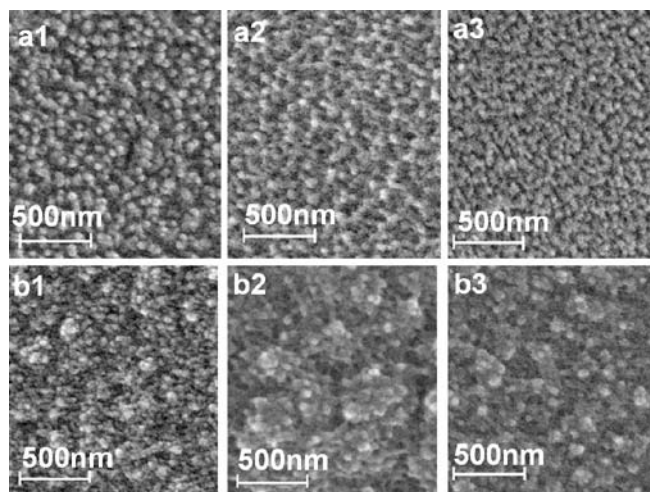
Fig. 1 SEM micrographs of polyaniline on Pt (*1*), Au (*2*), and C (*3*) substrates via three-step (**a**) and one-step (**b**) deposition. Electrolyte, a 0.5 M H_2SO_4/0.5 M aniline solution. The optimized three-step deposition procedure was set at 0.02 mA cm^{-2} for 0.5 h, 0.01 mAcm^{-2} for 3 h, and 0.005 mA cm^{-2} for 8 h. The conventional one-step method was performed by applying 0.02 mA cm^{-2} for 4 h

three-step method. For each 500×500 nm^2 region of the SEM image, about 30 to 40 well-orientated nanowires were observed where the white spots are actually the tips of uniform nanowires, mostly oriented perpendicular with respect to the substrates. The diameters of the tips range from 30 to 50 nm, while the slightly gray cylinders represent the bodies of the formed nanowires with estimated lengths of about 100~200 nm when viewed from the tilted angle. The interspaces of the nanowires ranging from about 30 to 80 nm are thus generated on the substrates, which can be treated as nanoporous channels for ion diffusion or transfer. The mechanism for the formation of such unique PANI nanowires is proposed as the nucleation and aggregation trisected by stepwise deposition. Such morphologies were expected to provide higher surface areas and would make the access of ions in the electrolyte in the electrode surface more easy than PANI obtained by the one-step method. On the contrary, the

PANI films generated by the latter only appeared as amorphous structures with random aggregated islands of large size-distribution in the range from several to hundreds of nanometers as illustrated in Fig. 1. It was reported that the polyaniline morphology has important effect on the electrochemical properties of polyaniline supercapacitors [16, 17] and then the electrochemcial properties of these PANI supercapacitors by three-step and one-step methods were also investigated and compared by AC electrochemical impedance spectroscopy (EIS), CV, and galvanostatic charge/discharge cycling techniques in the following parts.

EIS of PANI via three-step and one-step methods

EIS was employed to monitor the electrochemical behavior of the PANI electrodes. The low-frequency capacitance (C_{LF}) of PANI with different morphologies was determined from the slope of the imaginary component of impedance (Z'') at low frequency as shown in Fig. 2. Impedance data below 1 Hz were selected as usual to measure C_{LF}, as defined in Eq. 1 [3]:

$$C_{LF} = (2\pi f Z'')^{-1} \quad (1)$$

where Z'' was the imaginary impedance of the system at the frequency f. This equation is valid for low frequency when the impedance is almost purely capacitive. The value of C_{LF} was calculated at the point of $f=10$ mHz and listed in Table 1 in which C_{LF} for PANI prepared via three-step on Pt, Au, and C substrates clearly showed about three times larger than those obtained via one-step.
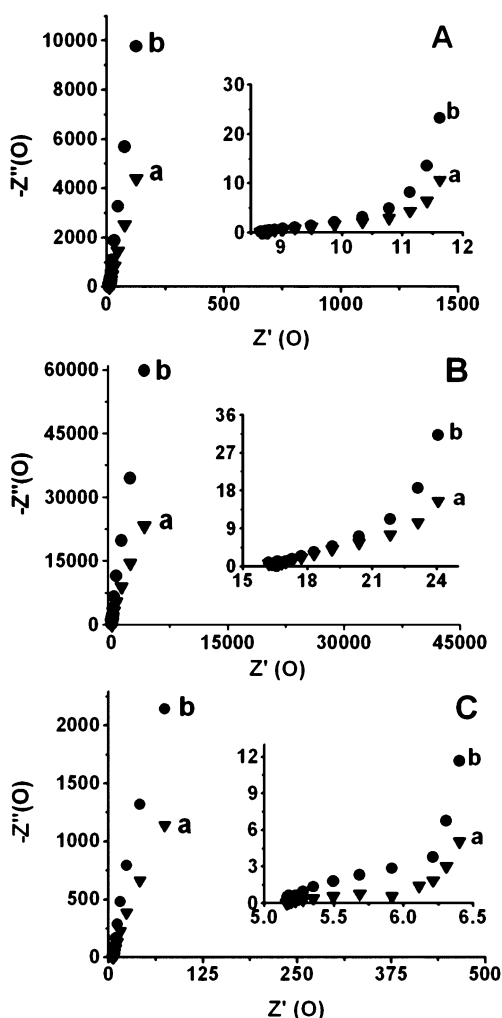
Fig. 2 Impedance Nyquist plots of PANI on Pt (*A*), Au (*B*), and C (*C*) substrates via three-step (**a**) and one-step (**b**) methods in a 0.5 M H$_2$SO$_4$ electrolyte solution. The high-frequency part was zoomed as the inset. The potential perturbation amplitude was fixed at 5 mV in the open-circuit potential. Frequencies range from 100 kHz to 10 mHz

Table 1 Capacitances for different types of PANI films

Types	Synthesis method	C_{LF} (F/g)	C_S (F/g)	C_P (F/g)	Ref
PANI/Pt	3-step	344	415	596	This work[a]
	1-step	119	157	189	
PANI/Au	3-step	314	419	541	
	1-step	122	155	129	
PANI/Carbon	3-step	330	437	589	
	1-step	176	181	234	
PANI/Carbon[b]	1-step	150	–	–	[10]
PANI/SWNT/Ni[c]	Chem.	–	–	190	[13]
PANI/Al[d]	Chem.	–	–	107	[11]
PANI/Carbon[e]	CV	–	–	180	[12]

[a] Capacitances measured in this work, all data are the average of three times the measurement with RSD less than 5%
[b] Prepared by galvanostatic deposition
[c] By chemical polymerization
[d] By chemically synthesized PANI powder
[e] By cyclic voltammetry

CV measurements of PANI via three-step and one-step methods

CV measurements were further performed in a potential range from 0.1 to 0.7 V to analyze the electrochemical behavior of the resulting electrodes in 0.5 M H_2SO_4 solution. The voltammograms of the PANI electrode via three-step and one-step methods are shown in Fig. 3. The voltammograms of all PANI electrodes appeared nearly rectangular in shape and no obvious redox peaks were observed, which suggested that the formed films would have a superior capacitive properties [3]. In addition, the currents of both the anodic and the cathodic half-cycles for PANI films via three-step were much larger than those formed by one-step, also, the total charges for the oxidation and reduction process, which implied that the ordered structures of the films by this novel method, might greatly enhance their capacitances.
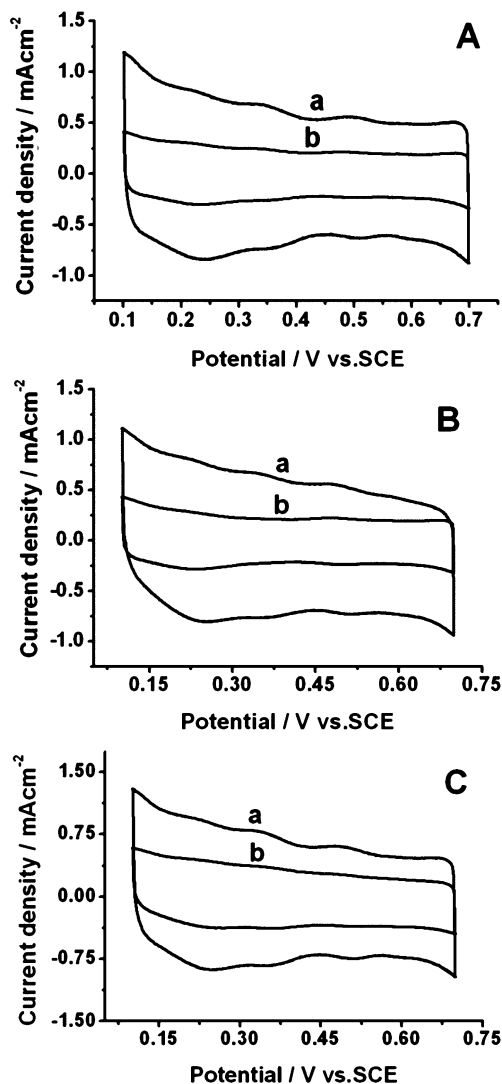

Fig. 3 Cyclic voltammograms of PANI on Pt (*A*), Au (*B*), and C (*C*) substrates via three-step (**a**) and one-step (**b**) methods in a 0.5 M H_2SO_4 electrolyte solution. Scan rate, 5 mV/s. Potential ranges, 0.1 to 0.7 V. Other conditions were the same as in Fig. 1
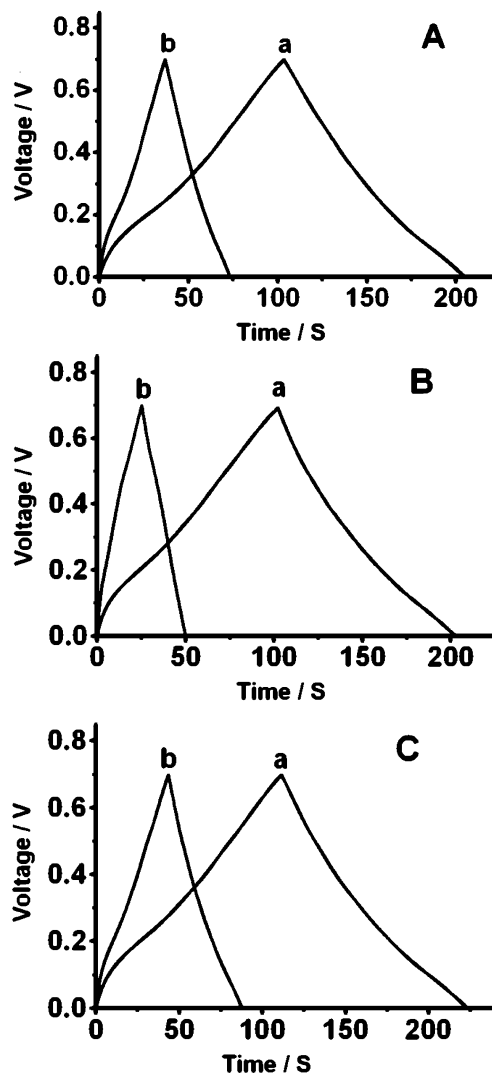

Fig. 4 Galvanostatic charge/discharge curves of polyaniline on Pt (*A*), Au (*B*), and C (*C*) substrate via three-step (**a**) and one-step (**b**) methods in a 0.5 M H_2SO_4 electrolyte solution. Current density of 1 mA cm^{-2}. Potential ranges, 0 to 0.7 V for 1,000 cycling times

The specific capacitance C_s was then measured and further calculated from the voltotammetric curves following the Eq. 2 [15]:

$$C_s = i/\nu \qquad (2)$$

where *i* is the average current response and *v* is the potential sweep rate. As displayed in Table 1, the remarkably increased C_s was observed for PANI via three-step than that for one-step.

Galvanostatic charge/discharge analysis of PANI via three-step and one-step methods

When using galvanostatic charge/discharge analysis to determine capacitance, the advantage of the PANI via three-stepwise growth was further emphasized. The volt-
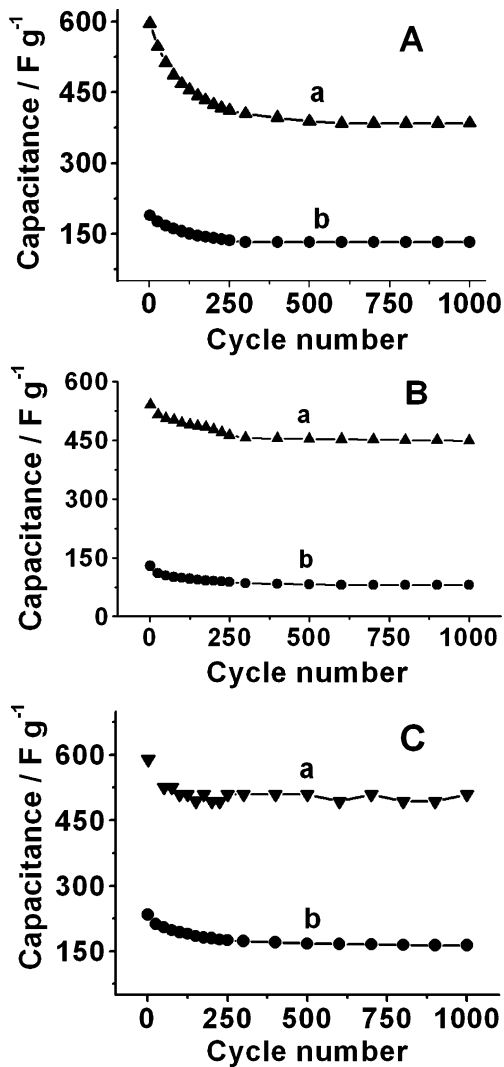
Fig. 5 Cycle life data of polyaniline on Pt (*A*), Au (*B*), and C (*C*) substrate via three-step (**a**) and one-step methods (**b**) in a 0.5 M H₂SO₄ electrolyte solution. Other conditions were the same as in Fig. 4

Table 2 BET analysis for PANI on Pt via three-step and one-step methods

	Descriptions	3-step	1-step
Area (m^2/g)	BET surface area	3.4294	0.6560
	Langmuir surface area	4.3898	0.8703
	Micropore area	0.7818	1.7918
	External surface area	2.6476	−1.1359
Volume (cm^3/g)	Micropore volume	0.000291	0.000781
Pore size (nm)	Adsorption Average pore diameter	38.1198	89.1269

BET results of PANI via three-step and one-step methods

The subsequent BET analysis showed that the surface areas for PANI via the two methods are quite different as shown in Table 2, e.g., 3.3 m^2/g and 0.64 m^2/g for PANI on Pt via three-step and one-step, respectively, surely verifying the above-mentioned assumption. Obviously, the greatly increased surface area supplies more charge storage capacity for charge and discharge process. Therefore, the performances, i.e., the charge capacity, the reversibility, and the stability, of the thus-obtained electrodes via three-step are reasonably enhanced, corresponding to the effect resulting from the BET surface areas.

Conclusions

In conclusion, the ordered polyaniline nanowires created by stepwise electrochemical deposition were shown to have remarkably increased capacitances several times higher than that by one-step method. The improved superior conductive performance can be mainly attributed to the increased BET surface areas and the formed ordered nanoporous structures, which would open a new way in designing of highly efficient electrochemical super capacitors or energy storage devices.

age variation of different morphologies in charge/discharge was shown in Fig. 4, and the specific discharge capacitance (C_p) of PANI was evaluated via Eq. 3 [1]:

$$C_p = It/Vm \qquad (3)$$

where I was the discharge current, t was the discharge time, V was the charge voltage (0.7 V), and m was the mass of PANI. The capacitance variations in the charge/discharge circles are displayed in Fig. 5 in which the PANI via three-step showed ideal stability and reversibility, typically for PANI on Au, ~20% loss of C_p was observed after 1,000 cycles. Here, Table 1 was presented to compare the capacitive properties of PANI-based electrodes in this work and in references. Again, the greatly increased capacitances corresponding to the improved PANI structure via three-step were clearly demonstrated.

References

1. An KH, Kim WS, Park YS, Choi YC, Lee SM, Chung DC, Bae DJ, Lim SC, Lee YH (2001) Adv Mater 13:497
2. Niu CM, Sichel EK, Hoch R, Moy D,Tennent H (1997) Appl Phys Lett 70:1480
3. Hughes M, Shaffer MSP, Renouf AC, Singh C, Chen GZ, Fray DJ, Windle AH (2002) Adv Mater 14:382
4. Teng H, Chang YJ, Hsieh CT (2001) Carbon 39:1981
5. Zhang JR, Jiang DC, Chen B, Zhu JJ, Jiang LP, Fang HQ (2001) J Electrochem Soc 148:A1362
6. Hu CC, Chang KH (2002) J Power Sources 112:401
7. Park JH, Park OO (2002) J Power Sources 109:121

8. Hu CC, Chang KH (2000) Electrochim Acta 45:2685
9. Rudge A, Raistrick I, Gottesfeld S, Frraris JP (1994) Electrochim Acta 39:273
10. Fusalba F, Gouerec P, Villers D, Belanger D (2001) J Electrochem Soc 148:A1
11. Ryu KS, Kim KM, Park NG, Park YJ, Chang SH (2002) J Power Sources 103:305
12. Chen WC, Wen TC, Teng HS (2003) Electrochim Acta 48:641
13. Zhou YK, He BL, Zhou WJ, Huang J, Li XH, Wu B, Li HL (2004) Electrochim Acta 49:257
14. Gomez-Romero P, Chojak M, Cuentas-Gallegos K, Asensio JA, Kulesza PJ, Casan-Pastor N, Lira-Cantu M (2003) Electrochem Commun 5:149
15. Park JH, Park OO (2002) J Power Sources 111:185
16. Neves S, Polo Fonseca C, Zoppi R, Córdoba de Torresi S (2001) J Solid State Electrochem 5:412
17. Zhou H, Chen H, Luo SL, Lu GW, Wei WZ, Kuang YF (2005) J Solid State Electrochem 9:574
18. (a) Liu J, Lin YH, Liang L, Voigt JA, Huber DL, Tian ZR, Coker E, Mckenzie B, Mcdermott MJ (2003) Chem Eur J 9:605. (b) Liang L, Liu J, Windisch CF, Exarhos GJ Jr, Lin YH (2002) Angew Chem 114:3817